

## Long-Term Stable Expression of Human Apolipoprotein A-I Mediated by Helper-Dependent Adenovirus Gene Transfer Inhibits Atherosclerosis Progression and Remodels Atherosclerotic Plaques in a Mouse Model of Familial Hypercholesterolemia

L. Maria Belalcazar, MD\*; Aksam Merched, PhD\*; Boyd Carr; Kazuhiro Oka, PhD; Kuang-Hua Chen, PhD; Lucio Pastore, MD, PhD; Arthur Beaudet, MD; Lawrence Chan, MBBS, DSc

**Background**—Epidemiologic studies and transgenic mouse experiments indicate that high plasma HDL and apolipoprotein (apo) A-I protect against atherosclerosis. We used helper-dependent adenovirus (HD-Ad) gene transfer to examine the effect of long-term hepatic apoA-I expression on atherosclerotic lesion progression and remodeling in a mouse model of familial hypercholesterolemia.

**Methods and Results**—We treated LDL receptor-deficient (LDLR<sup>-/-</sup>) mice maintained on a high-cholesterol diet for 6 weeks with either a HD-Ad containing human apoA-I gene (HD-Ad-AI) or saline (control). HD-Ad-AI treatment did not affect plasma liver enzymes but induced the appearance of plasma human apoA-I at or above human levels for the duration of the study. Substantial amounts of human apoA-I existed in lipid-free plasma. Compared with controls, HDLs from treated mice were larger and had a greater inhibitory effect on tumor necrosis factor- $\alpha$ -induced vascular cellular adhesion molecule-1 expression in cultured endothelial cells. Twenty-four weeks after injection, aortic atherosclerotic lesion area in saline-treated mice progressed  $\approx$ 700%; the rate of progression was reduced by >50% by HD-Ad-AI treatment. The lesions in HD-Ad-AI-treated mice contained human apoA-I that colocalized mainly with macrophages; they also contained less lipid, fewer macrophages, and less vascular cellular adhesion molecule-1 immunostaining but more smooth muscle cells ( $\alpha$ -actin staining) and collagen.

**Conclusions**—HD-Ad-AI treatment of LDLR<sup>-/-</sup> mice leads to long-term overexpression of apoA-I, retards atherosclerosis progression, and remodels the lesions to a more stable-appearing phenotype. HD-Ad-mediated transfer of apoA-I may be a useful clinical approach for protecting against atherosclerosis progression and stabilizing atherosclerotic lesions associated with dyslipidemia in human patients. (*Circulation*. 2003;107:2726-2732.)

**Key Words:** gene therapy ■ apolipoproteins ■ hypercholesterolemia ■ atherosclerosis ■ adenovirus

Low HDL cholesterol is the most frequent lipid disorder in patients with coronary artery disease.<sup>1</sup> Apolipoprotein A-I (apoA-I) is a major protein component of HDL and plays a pivotal role in its formation. ApoA-I level seems to be a better indicator of coronary risk than HDL cholesterol level.<sup>2</sup> Animal studies have demonstrated that elevated plasma apoA-I by protein infusion<sup>3</sup> or transgenic overexpression<sup>4-7</sup> protects against atherosclerotic progression and may induce lesion regression.

Given the protective role of the *APOAI* gene, somatic gene transfer of apoA-I is an attractive strategy for the treatment of atherosclerotic disease. For hepatic transgene

expression, adeno-associated virus (AAV) and helper-dependent adenovirus (HD-Ad) are presently the most promising vehicles for experimental gene therapy. AAV is relatively nontoxic but has relatively low transduction efficiency and cloning capacity. For proteins that require high plasma concentrations (in the 1 mg/mL range) to be effective, HD-Ads may be preferred. HD-Ads lack all viral protein coding sequences and seem to be substantially less toxic than earlier generation Ads. They have been reported to express transgenes in vivo in a stable and effective manner.<sup>8-13</sup> These advantages and a natural tropism of this vector to the liver prompted us to test the efficacy of

Received November 5, 2002; revision received February 20, 2003; accepted February 28, 2003.

From the Department of Medicine (L.M.B., B.C.), University of Texas Medical Branch, Galveston, Tex; Departments of Medicine and Molecular & Cellular Biology (L.M.B., A.M., K.O., K.-H.C., L.C.) and Molecular & Human Genetics (L.P., A.B.), Baylor College of Medicine, Houston, Tex; and St Luke's Episcopal Hospital (L.C.), Houston, Tex.

Guest editor for this article was Peter Libby, MD, Brigham and Women's Hospital, Boston, Mass.

\*These authors contributed equally to this study.

Correspondence to Dr Lawrence Chan, Department of Medicine, Section of Endocrinology & Metabolism, Baylor College of Medicine, One Baylor Plaza, Houston, TX 77030. E-mail lchan@bcm.tmc.edu

© 2003 American Heart Association, Inc.

*Circulation* is available at <http://www.circulationaha.org>

DOI: 10.1161/01.CIR.0000066913.69844.B2

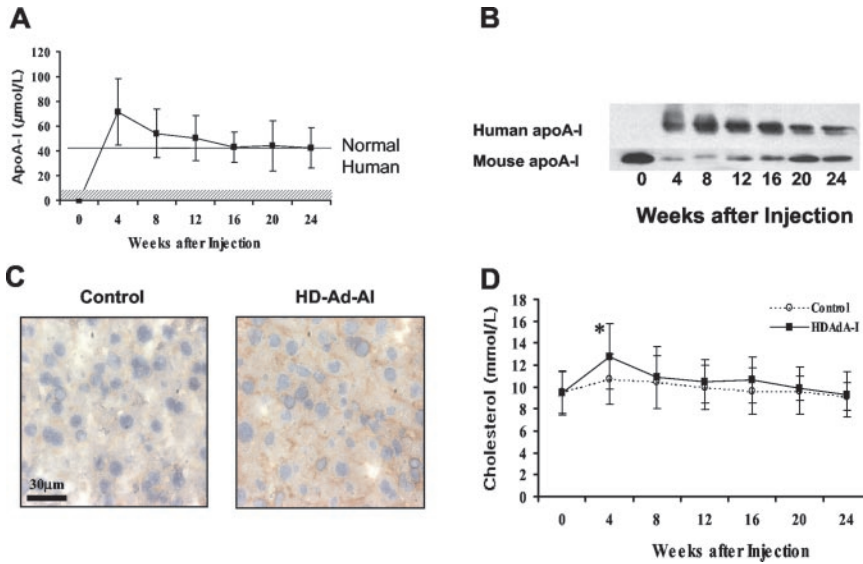


**Figure 1.** Characterization of plasma apoA-I and cholesterol. A, Human apoA-I levels in treated mice. The hatched bar at the bottom of the graph represents the level of cross-reactivity of the antibody with mouse apoA-I. B, Western blots of apoA-I in plasma of HD-Ad-AI-treated mice. C, Immunostaining of human hepatic apoA-I 4 weeks after a single injection of HD-Ad-AI or saline. D, Plasma cholesterol levels in HD-Ad-AI-treated mice and controls. \**P*<0.01.

HD-Ad-mediated apoA-I gene transfer in the treatment of progressive atherosclerotic disease.

**Methods**

**Construction and Evaluation of HD-Ad-AI**

An 11-kb *Eco*R1 fragment containing the human apoA-I gene<sup>14</sup> was first subcloned into a pLPBL1 vector<sup>15</sup> and then into pΔ21.<sup>13</sup> Rescue and amplification of the HD-Ad-AI were performed by the method of Parks et al.<sup>9</sup> The vector was characterized as described previously.<sup>15</sup>

**Animal Studies**

Animal studies were performed according to Baylor College of Medicine institutional guidelines. Female LDL receptor-deficient (LDLR<sup>-/-</sup>) mice on a C57BL/6 background (Jackson Laboratory) were started on a laboratory chow supplemented with 0.2% (wt/wt) cholesterol and 10% coconut oil (vol/wt) at 6 to 9 weeks of age. Six weeks later, a subgroup of mice (n=10) was killed, and the baseline en face aortic lesion size was determined. Thirty-eight mice were then injected via tail vein with HD-Ad-AI (4.5×10<sup>12</sup> particles/kg) and 36 mice with an equivalent volume of saline (200 µL). Animals were followed for up to 24 weeks after injection (30 weeks of high-cholesterol diet). Subgroups of animals were killed for quantification of lesions and histological evaluation at 4, 12, and 24 weeks after injection. Blood was collected monthly from the retro-orbital

plexus into EDTA-containing tubes after a 5-hour fast and immediately centrifuged to obtain plasma, which was stored at -20°C or at 4°C for analyses.

**Immunohistochemistry, Histology, and Quantitation of Atherosclerotic Lesions**

Immunohistochemical and histological studies were performed on fresh-frozen OCT-embedded proximal aortic sections (5 µm thick). For immunohistochemistry, slides were fixed in cold acetone. They were incubated with either monoclonal anti-human apoA-I or anti-α-actin (Biodesign, 1:100 and Sigma, 1:800, respectively), and the M.O.M. Basic Kit (Vector) was used for detection. Macrophages and vascular cell adhesion molecule-1 (VCAM-1) were detected by immunostaining with MOMA-2 (1:25) or anti-VCAM-1 (1:100) antibody (PharMingen) using Dako EnVision AP or HRP polymer system and a rat-specific kit (Vector). Histology was performed using standard techniques for Oil-Red O, H&E, trichrome, and Van Kossa. Aortic en face lesions were evaluated by quantitative morphometry as previously described.<sup>15</sup> VCAM-1-positive area was assessed in 3 to 4 serial 10-µm sections at 70-µm intervals. After capturing images of the aortic sections, we determined VCAM-1-positive area by computer-assisted color-gated measurement on the total lesion area (SigmaScanPro 5, SPSS).

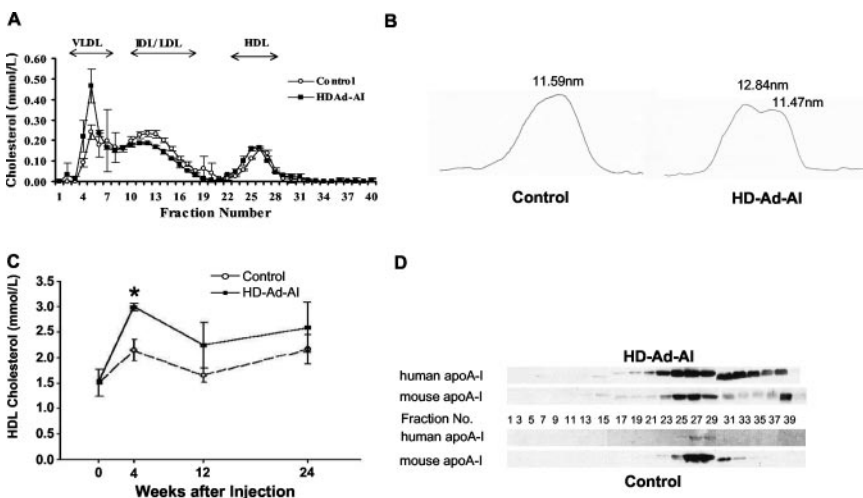


**Figure 2.** FPLC analysis. A, FPLC profile of total plasma cholesterol. Plasma was collected from mice 4 weeks after injection. B, Profiles of HDL fractions from saline-treated (control) and HD-Ad-AI-treated mice obtained from nondenaturing gradient gel scans 16 weeks after virus injection. C, HDL cholesterol levels in HD-Ad-AI-treated mice and controls. \**P*<0.01, †*P*<0.05. D, ApoA-I immunoblot analysis of FPLC fractions. Fractions were concentrated with fused silica before analyses. The signal of human apoA-I immunoreactive protein in control mice reflects the cross-reactivity of anti-human apoA-I antibody to the mouse apoA-I.

## HDL Modulation of Tumor Necrosis Factor- $\alpha$ -Induced VCAM-1 Expression in Cultured Endothelial Cells

The effect of HDL isolated from control or HD-Ad-AI-treated mice on tumor necrosis factor- $\alpha$  (TNF- $\alpha$ )-induced VCAM-1 expression was tested in cultured human umbilical vein endothelial cells (HUVECs). HDL was isolated by sequential ultracentrifugation using a TL-100 Beckman ultracentrifuge.<sup>16</sup> The purity of fractions was confirmed by lipoprotein agarose electrophoresis. HUVECs were cultured in 96-well tissue culture plates until a density of  $1.0 \times 10^4$  cells/well was reached and then incubated with 0.1 mL of HDL in the presence of 50 U/mL TNF- $\alpha$  (Boehringer Mannheim). HUVEC VCAM-1 expression was determined 3 hours after incubation by ELISA.<sup>17</sup>

### Statistical Analysis

Data for lesions and VLDL, IDL/LDL, and HDL cholesterol were analyzed by two-way ANOVA with factors time (0, 4, 12, and 24 weeks) and treatment group (HD-Ad-AI versus control). Plasma cholesterol levels were compared across time, within a group by paired *t* test. Comparisons between groups for plasma lipids and induced VCAM-1 expression were performed by a 2-sample *t* test. The Wilcoxon rank-sum test was used when appropriate to confirm normality.

### Other Procedures

Lipids and FPLC (Amersham Pharmacia Biotech AB) analyses were performed as previously described.<sup>18</sup> Human plasma apoA-I levels were quantitated by an immunoturbidimetric assay (Diasorin). HDL cholesterol was determined from FPLC fractions. Three sets of pooled plasma (200  $\mu$ L) from control and HD-Ad-AI-treated mice were used for these determinations. For immunoblot analysis, plasma was diluted 1:32, electrophoresed on a 12% SDS-polyacrylamide gel, and transferred to membrane, which was then incubated either with a goat anti-human apoA-I antibody (1:2000 dilution, Chemicon) or with a rabbit anti-mouse apoA-I antibody (1:100 dilution, Biodesign). Immunoreactive proteins were detected by ECL (Amersham Pharmacia Biotech). For HDL particle sizing, the lipoprotein fraction was isolated as described above and subjected to nondenaturing electrophoresis on a 4% to 20% polyacrylamide gradient gel. Computer-assisted densitometry with coelectrophoresed molecular size calibrators was used to determine particle size.

## Results

### Effect of HD-Ad-AI on Total Plasma Cholesterol and ApoA-I in LDLR<sup>-/-</sup> Mice

HD-Ad-AI vector was characterized by Southern blot analysis, which showed <0.2% helper virus contamination and no detectable DNA rearrangement (data not shown). LDLR<sup>-/-</sup> mice maintained on an atherogenic diet for 6 weeks had a basal plasma cholesterol of  $9.49 \pm 2.02$  mmol/L ( $368 \pm 74$  mg/dL). A single injection ( $4.5 \times 10^{12}$  particles/kg) of HD-Ad-AI led to the appearance of human apoA-I in plasma, which reached a peak of  $71.4 \pm 26.6$   $\mu$ mol/L ( $200 \pm 75$  mg/dL) at 4 weeks. Plasma liver enzymes remained similar in saline and HD-Ad-AI-treated mice (data not shown). The level of apoA-I (42.9  $\mu$ mol/L) in treated mice remained at or above the normal human range for 24 weeks after injection (Figure 1A). Appearance of human apoA-I in plasma led to a drop in mouse apoA-I concentration in plasma (Figure 1B). Immunohistochemical staining confirmed the expression of human apoA-I in the liver (Figure 1C). Plasma total cholesterol level at the time of the injection was  $9.49 \pm 2.02$  mmol/L. It increased to  $12.77 \pm 2.97$  mmol/L at 4 weeks and stabilized

approximately to control level thereafter (10.34 mmol/L, Figure 1D).

### Effect of HD-Ad-AI Treatment on Plasma HDL

We characterized the plasma lipoproteins of HD-Ad-AI-treated mice by FPLC. We noted a small but significant increase in the VLDL fraction and a minor lowering of the IDL/LDL peak in HD-Ad-AI-treated mice (Figure 2A). Interestingly, there was little difference in the HDL peak height; there was, however, a shift of the HDL peak to the left, indicating that these animals' HDL particles were larger than those in controls. We confirmed this size difference by nondenaturing gradient gel electrophoresis (Figure 2B). There was a significant increase in total plasma HDL cholesterol in HD-Ad-AI mice compared with controls at 4 weeks (Figure 2C). We additionally studied the distribution of apoA-I in the FPLC fractions (Figure 2D). In saline-treated mice, essentially all of the mouse apoA-I was found in the HDL fraction. In contrast, a substantial portion of human

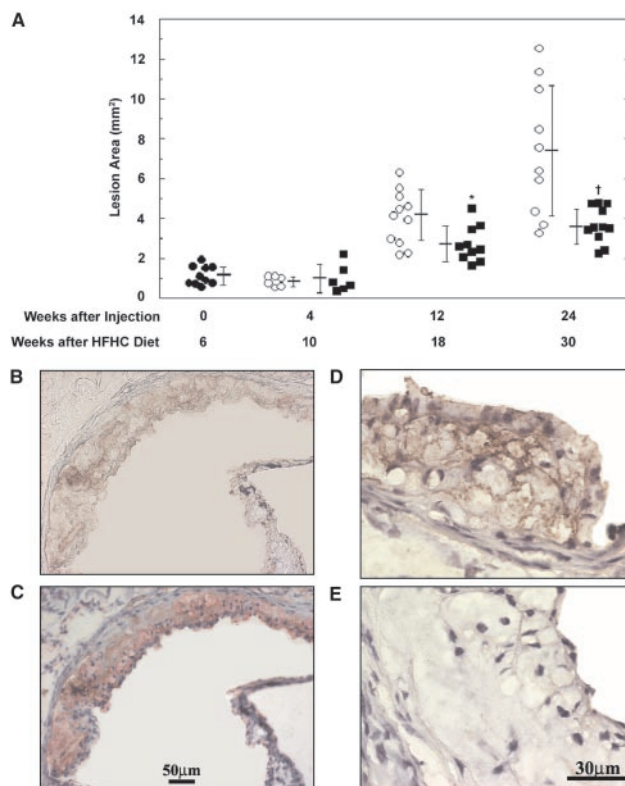


**Figure 3.** Aortic lesion analyses. A, En face quantification of aortic lesions. ●, Saline-treated mice (control) at baseline (before injection); ○, Saline-treated mice; ■, HD-Ad-AI treated mice. \* $P \leq 0.015$ , † $P \leq 0.008$  (HD-Ad-AI-treated versus control mice at the indicated time). B, Cross-section of aorta in an HD-Ad-AI-treated mouse 8 weeks after injection (seen with  $\times 200$  magnification). Human apoA-I appears in brown without counterstaining. C, Same aortic cross-section as in B with a second immunostaining for macrophage-derived (MOMA-2-positive, bright red) cells. We observed the colocalization of apoA-I staining in macrophage-positive areas. D, Human apoA-I immunostaining (brown) in aortic cross-section of an HD-Ad-AI-treated mouse (seen with  $\times 630$  magnification); apoA-I is detected intracellularly and between cells. E, Absence of human apoA-I immunostaining in a cross-section of aorta from a control mouse.

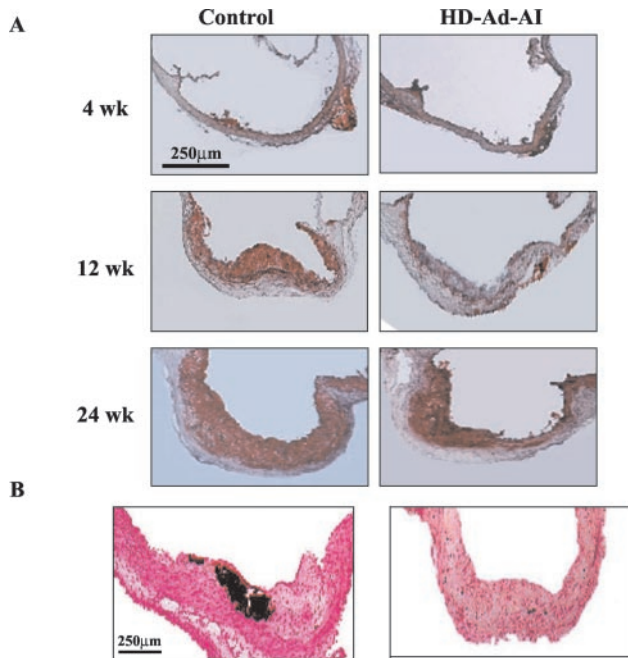


**Figure 4.** Progression of atherosclerotic lesions to an advanced stage in  $LDLR^{-/-}$  mice. A, Oil-Red O staining of aortic cross-sections. Bright red represents lipid deposition. Note extensive fat deposits in the subintimal area in the control mice at 24 weeks after injection. B, Van-Kossa staining of aortic cross-sections at 24 weeks. Black staining identifies calcium deposits within the lesions.

apoA-I was found in the lipoprotein-free fraction of HD-Ad-AI-treated mice (about half of the human apoA-I). HDL has been shown to modulate the expression of adhesion molecules on vascular endothelial cells.<sup>19,20</sup> We examined the effect of HDL on TNF- $\alpha$ -stimulated VCAM-1 expression in HUVECs in vitro. HDL isolated from saline-treated mice had little or no effect on TNF- $\alpha$ -stimulated VCAM-1 expression in these cells; however, HDL isolated from HD-Ad-AI mice at 4 or 24 weeks strongly inhibited VCAM-1 expression ( $55 \pm 6\%$  and  $56 \pm 3\%$  inhibition, respectively;  $n=3$ ;  $*P<0.001$  versus TNF- $\alpha$  alone). The culture medium contained 55.0 and 31.4  $\mu\text{mol/L}$  human apoA-I, respectively, for the 4- and 24-week incubations.

### Effect of HD-Ad-AI Treatment on Atherosclerosis Development in $LDLR^{-/-}$ Mice

En face lesion analysis demonstrated no difference between the two groups at 4 weeks. At 12 weeks, there was a 34% decrease in mean lesion area in the HD-Ad-AI-treated mice compared with saline-treated controls. The protective effect of apoA-I was even stronger at 24 weeks, when lesion area in the HD-Ad-AI-treated mice was reduced by 50% (Figure 3A). Immunoreactive human apoA-I was localized in the intracellular compartment and colocalized with markers of macrophage lineage, suggesting that it is present within foam cells of macrophage origin (Figures 3B through 3E).

Histology at sequential time points (Figures 4 and 5) demonstrates progression of atherosclerotic lesions from scant intimal fat deposits compatible with type I lesions to complex lesions analogous to type IV and V lesions in

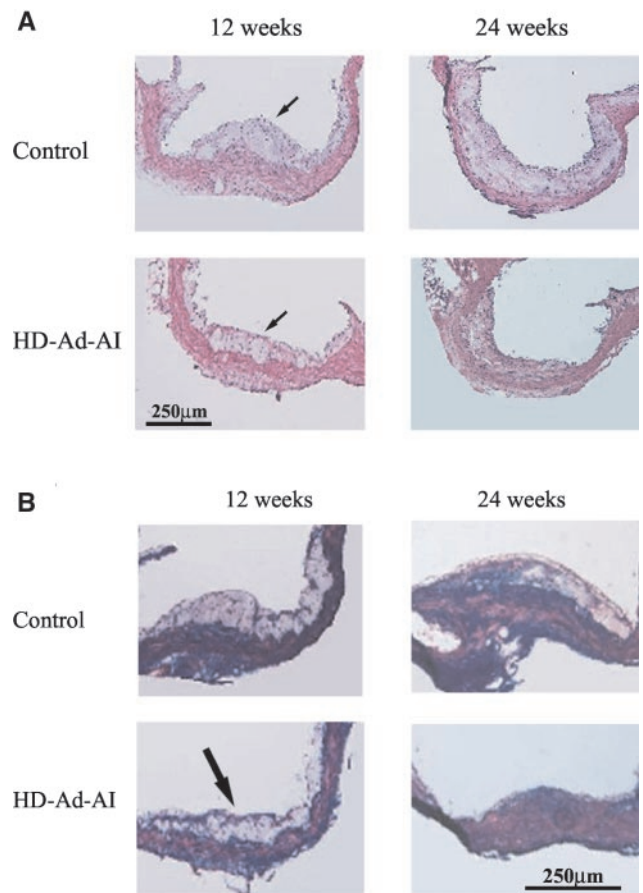


**Figure 5.** Histologic features of atherosclerotic lesions in HD-Ad-AI-treated and saline-treated mice. A, H&E staining of aortic cross-sections. Note formation of fatty streaks in both saline-treated and HD-Ad-AI-treated mice at 12 weeks (arrow). Lesions in the HD-Ad-AI-treated mice show formation of a lesion cap. At 24 weeks, saline-treated mice show substantial disruption of the subendothelium. B, Trichrome staining of aortic cross-sections. Collagen over lesion area in treated mice is depicted in blue (arrow). At 24 weeks, the distribution of collagen within the vessel wall is uniform and distinct in the HD-Ad-AI-treated mice, in contrast to controls.

humans.<sup>21,22</sup> No significant difference between the two groups was observed at 4 weeks. At 12 weeks after injection, compared with control mice, the treated mice showed a decrease in foam cells and lipid deposition and a more pronounced fibrotic response. The difference in lipid deposition was even more evident at 24 weeks (30 weeks of high-cholesterol diet). Lesions in control mice showed marked extracellular lipid accumulation, extensive calcium deposits, and disorganization of the collagen-rich extracellular matrix with atheromatous complications in the deep intima. In contrast, treated mice displayed decreased lipid deposition, scant calcium deposits, and a preservation of collagen-rich extracellular matrix integrity suggestive of greater plaque stability.

Immunohistochemistry reveals plaque-stabilizing features in the HD-Ad-AI-treated mice compared with controls (Figure 6). At 8 weeks after treatment, we observed deposition of human apoA-I in plaques of HD-Ad-AI-treated mice but relatively little difference in the distribution of  $\alpha$ -actin stain-

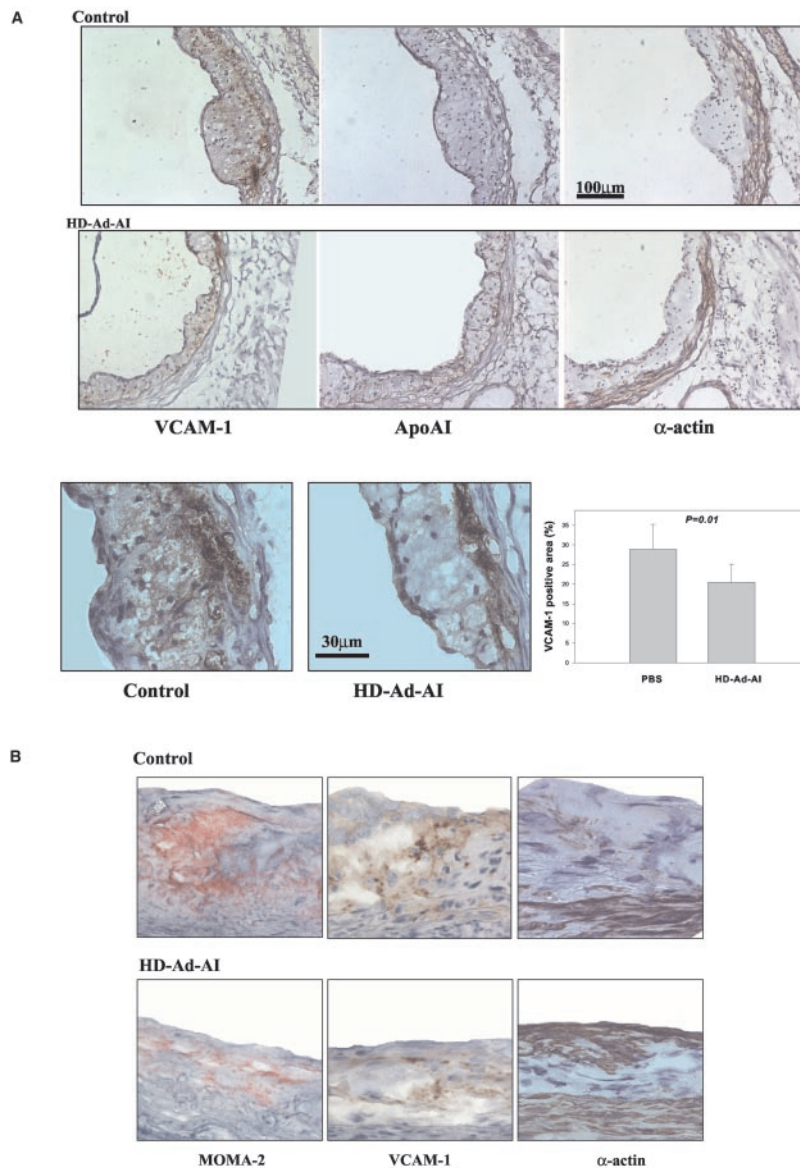


**Figure 6.** Immunostaining for  $\alpha$ -actin, apoA-I, MOMA-2, and VCAM-1 in atherosclerotic lesions 8 weeks (A) and 24 weeks (B) after vector injection. A, VCAM-1, human apoA-I, and  $\alpha$ -actin are stained brown. Bottom left, VCAM-1 immunostaining (brown) at higher magnification ( $\times 630$ ). Bottom right, Morphometric analysis of VCAM-1 staining. In the histogram, VCAM-1-positive area was determined by computer-assisted measurement and expressed as a percentage of total lesion area per section. B, From left to right: immunostaining of MOMA-2 (macrophage staining, red), VCAM-1 (brown), and  $\alpha$ -actin (dark brown) in aortic lesions 24 weeks after treatment with saline (top) or HD-Ad-AI (bottom).

ing between treated and control mice (Figure 6A). Even at this early stage, however, there was a clear reduction in VCAM-1 immunostaining (an indirect marker of inflammation) in the plaques of HD-Ad-AI-treated mice compared with controls. VCAM-1 staining was more intense over  $\alpha$ -actin staining (smooth muscle) cells. Quantitative morphometry confirmed that VCAM-1-positive area was reduced in the lesion of HDAd-AI-treated mice (Figure 6A, bottom). At 24 weeks after HD-Ad-AI treatment, in addition to a persistent reduction in VCAM-1 staining (Figure 6B, middle), the amount of macrophage (MOMA-2) staining (Figure 6B, left) was also decreased, whereas smooth muscle staining ( $\alpha$ -actin, Figure 6B, right) was substantially increased in treated mice.

### Discussion

Two studies published previously in *Circulation* studied the effect of transient apoA-I gene transfer on atherosclerosis development in various mouse models<sup>23,24</sup> and concluded that

short-term hepatic apoA-I expression produced regression of aortic atherosclerosis. Benoit et al<sup>23</sup> used human apoA-I transgenic mice (with concomitant apoE deficiency) as a study model to obtain the longest possible transgene expression. With the first-generation Ad vector used, they had to terminate the experiment after 6 weeks when the transient apoA-I expression declined. They reported that the gene transfer “inhibited fatty streak lesion formation by 56%” (Benoit et al,<sup>23</sup> p 105). Tangirala et al<sup>24</sup> used a second-generation Ad vector in an LDLR<sup>-/-</sup> mice fed a high-fat high-cholesterol diet to produce plasma cholesterol averaging  $\approx 31$  mmol/L to induce massively accelerated fatty streak lesion formation. These authors found a remarkable 70% reduction in en face aortic atherosclerosis lesion area after only 4 weeks of treatment. However, as pointed out by an accompanying editorial,<sup>25</sup> the two studies only suggest that the gene transfer producing transiently elevated apoA-I can reduce the size of “preexisting lesions, at least those with complexity corresponding to American Heart Association

types I and II (ie, fatty streaks)" (Dansky and Fisher,<sup>25</sup> p 1762). These studies confirm the antiatherosclerotic potential of apoA-I, but the conclusions were limited by the short duration of apoA-I transgene expression, and the authors' analysis was applicable only to the effects of apoA-I on early-stage fatty streaks. In humans, early atherosclerotic lesions may be present in childhood, are clinically silent, and do not necessarily progress to advanced disease.<sup>21,22,26</sup> In fact, fatty streaks frequently regress spontaneously.<sup>26</sup> Therefore, the clinical relevance of the previous findings<sup>23,24</sup> is uncertain.

We believe that our observations on HD-Ad-AI gene transfer in the hypercholesterolemic mice are directly relevant if apoA-I gene therapy ever comes to clinical trials. We followed the effect of apoA-I overexpression until complex lesions developed ( $\approx$ 7 months into the study) and found that at this stage, its antiatherosclerotic potential is much more evident than at earlier time points during the disease process. Early on, when plasma apoA-I levels peaked at 4 weeks, there was no difference in lesion area between treated mice and controls. At this early time point, little human apoA-I was detected in the vascular wall. These observations suggest that the presence of apoA-I in the vessel wall may be exerting a direct effect on the cells of the lesion against atherosclerotic disease progression. The shift in the distribution of apoA-I toward smaller lipid-poor particles with HD-Ad-AI treatment (Figures 2A and 2D) might facilitate the access of apoA-I to the arterial intima.<sup>27</sup> In addition, there is evidence that human apoA-I may have greater antiatherogenic potential compared with mouse apoA-I.<sup>28</sup>

The expression of adhesion molecules on endothelial cells is thought to be an important component in atherogenesis.<sup>19,29</sup> TNF- $\alpha$ -induced-VCAM-1 expression in cultured HUVECs was significantly inhibited by the HDL isolated from HD-Ad-AI-treated mice but not from control mice, which suggests that one mechanism of the protective effects of HDL against development of atherosclerosis is inhibition of the interaction between leukocytes and endothelium.<sup>20</sup>

Immunohistochemical analysis demonstrated that apoA-I localized preferentially in the intracellular compartment of macrophage-derived foam cells (Figures 3B through 3D). In addition, HD-Ad-AI treatment led to a more stable-appearing plaque phenotype associated with a decrease in subendothelial lipid deposits and a reduction in macrophage-derived cells and adhesion molecule expression. We also observed an increase in smooth muscle cells on the surface of the lesions (Figures 4 through 6). Similar effects of high levels of plasma apoA-I on the remodeling of atherosclerotic lesions into a more stable-appearing phenotype have been observed in thoracic aortas transplanted from apoE-deficient mice to human apoA-I-overexpressing apoE-deficient mice.<sup>30</sup> The multifaceted beneficial effects of apoA-I on both lesion progression and remodeling strongly suggest that apoA-I gene therapy may be an effective way to inhibit lesion progression as well as to remodel atherosclerotic lesions into a phenotype that is associated with a lower probability of clinical events.<sup>24,31–34</sup>

In conclusion, changing the functional properties of plasma HDL by apoA-I gene transfer is an effective way to retard

atherosclerotic lesion progression as well as to transform such lesions into a more stable-appearing phenotype. Thus, apoA-I gene therapy using a HD-Ad vector is a promising approach for the treatment of patients with established atherosclerosis. Additional studies along these lines are warranted.

### Acknowledgments

This work was supported by grants HL-59314 and HL-16512 from the National Institutes of Health. Dr Merched was supported by Bayer-Pharma France, and Dr Chan was supported by the Betty Rutherford Chair in Diabetes and Endocrinology Research. We thank Merck & Co for providing reagents developed by F. Graham; E. Antonova, M. Merched-Sauvage, E.A. Nour, and C. Dieker for their technical assistance in the study; L. Muehlberger from University of Texas Medical Branch for her assistance with aortic histology; M. Finegold for help with histological examination of the liver; and M. Majesky for helpful comments on the manuscript.

### References

1. Kannel WB. Range of serum cholesterol values in the population developing coronary artery disease. *Am J Cardiol.* 1995;76:69C–77C.
2. Maciejko JJ, Holmes DR, Kottke BA, et al. Apolipoprotein A-I as a marker of angiographically assessed coronary-artery disease. *N Engl J Med.* 1983;309:385–389.
3. Miyazaki A, Sakuma S, Morikawa W, et al. Intravenous injection of rabbit apolipoprotein A-I inhibits the progression of atherosclerosis in cholesterol-fed rabbits. *Arterioscler Thromb Vasc Biol.* 1995;15:1882–1888.
4. Rubin EM, Krauss RM, Spangler EA, et al. Inhibition of early atherogenesis in transgenic mice by human apolipoprotein AI. *Nature.* 1991;353:265–267.
5. Paszty C, Maeda N, Verstuyft J, et al. Apolipoprotein AI transgene corrects apolipoprotein E deficiency-induced atherosclerosis in mice. *J Clin Invest.* 1994;94:899–903.
6. Plump AS, Scott CJ, Breslow JL. Human apolipoprotein A-I gene expression increases high density lipoprotein and suppresses atherosclerosis in the apolipoprotein E-deficient mouse. *Proc Natl Acad Sci U S A.* 1994;91:9607–9611.
7. Duverger N, Kruth H, Emmanuel F, et al. Inhibition of atherosclerosis development in cholesterol-fed human apolipoprotein A-I-transgenic rabbits. *Circulation.* 1996;94:713–717.
8. Kochanek S, Clemens PR, Mitani K, et al. A new adenoviral vector: replacement of all viral coding sequences with 28 kb of DNA independently expressing both full-length dystrophin and beta-galactosidase. *Proc Natl Acad Sci U S A.* 1996;93:5731–5736.
9. Parks RJ, Chen L, Anton M, et al. A helper-dependent adenovirus vector system: removal of helper virus by Cre-mediated excision of the viral packaging signal. *Proc Natl Acad Sci U S A.* 1996;93:13565–13570.
10. Schiedner G, Morral N, Parks RJ, et al. Genomic DNA transfer with a high-capacity adenovirus vector results in improved in vivo gene expression and decreased toxicity. *Nat Genet.* 1998;18:180–183.
11. Morral N, O'Neal W, Rice K, et al. Administration of helper-dependent adenoviral vectors and sequential delivery of different vector serotype for long-term liver-directed gene transfer in baboons. *Proc Natl Acad Sci U S A.* 1999;96:12816–12821.
12. Morral N, Parks RJ, Zhou H, et al. High doses of a helper-dependent adenoviral vector yield supra-physiological levels of alpha1-antitrypsin with negligible toxicity. *Hum Gene Ther.* 1998;9:2709–2716.
13. Kim IH, Jozkowicz A, Piedra PA, et al. Lifetime correction of genetic deficiency in mice with a single injection of helper-dependent adenoviral vector. *Proc Natl Acad Sci U S A.* 2001;98:13282–13287.
14. Rubin EM, Ishida BY, Clift SM, et al. Expression of human apolipoprotein A-I in transgenic mice results in reduced plasma levels of murine apolipoprotein A-I and the appearance of two new high density lipoprotein size subclasses. *Proc Natl Acad Sci U S A.* 1991;88:434–438.
15. Oka K, Pastore L, Kim IH, et al. Long-term stable correction of low-density lipoprotein receptor-deficient mice with a helper-dependent adenoviral vector expressing the very low-density lipoprotein receptor. *Circulation.* 2001;103:1274–1281.
16. Brousseau T, Clavey V, Bard JM, et al. Sequential ultracentrifugation micromethod for separation of serum lipoproteins and assays of lipids, apolipoproteins, and lipoprotein particles. *Clin Chem.* 1993;39:960–964.

17. Chen KH, Reece LM, Leary JF. Mitochondrial glutathione modulates TNF-alpha-induced endothelial cell dysfunction. *Free Radic Biol Med*. 1999;27:100-109.
18. Kobayashi K, Oka K, Forte T, et al. Reversal of hypercholesterolemia in low density lipoprotein receptor knockout mice by adenovirus-mediated gene transfer of the very low density lipoprotein receptor. *J Biol Chem*. 1996;271:6852-6860.
19. Libby P, Li H. Vascular cell adhesion molecule-1 and smooth muscle cell activation during atherogenesis. *J Clin Invest*. 1993;92:538-539.
20. Cockerill GW, Rye KA, Gamble JR, et al. High-density lipoproteins inhibit cytokine-induced expression of endothelial cell adhesion molecules. *Arterioscler Thromb Vasc Biol*. 1995;15:1987-1994.
21. Stary HC, Chandler AB, Glagov S, et al. A definition of initial, fatty streak, and intermediate lesions of atherosclerosis: a report from the Committee on Vascular Lesions of the Council on Arteriosclerosis, American Heart Association. *Arterioscler Thromb*. 1994;14:840-856.
22. Stary HC, Chandler AB, Dinsmore RE, et al. A definition of advanced types of atherosclerotic lesions and a histological classification of atherosclerosis: a report from the Committee on Vascular Lesions of the Council on Arteriosclerosis, American Heart Association. *Arterioscler Thromb Vasc Biol*. 1995;15:1512-1531.
23. Benoit P, Emmanuel F, Caillaud JM, et al. Somatic gene transfer of human ApoA-I inhibits atherosclerosis progression in mouse models. *Circulation*. 1999;99:105-110.
24. Tangirala RK, Tsukamoto K, Chun SH, et al. Regression of atherosclerosis induced by liver-directed gene transfer of apolipoprotein A-I in mice. *Circulation*. 1999;100:1816-1822.
25. Dansky HM, Fisher EA. High-density lipoprotein and plaque regression: the good cholesterol gets even better. *Circulation*. 1999;100:1762-1763.
26. Virmani R, Kolodgie FD, Burke AP, et al. Lessons from sudden coronary death: a comprehensive morphological classification scheme for atherosclerotic lesions. *Arterioscler Thromb Vasc Biol*. 2000;20:1262-1275.
27. Tall AR. Plasma high density lipoproteins: metabolism and relationship to atherogenesis. *J Clin Invest*. 1990;86:379-384.
28. Castro G, Nihoul LP, Dengremont C, et al. Cholesterol efflux, lecithin-cholesterol acyltransferase activity, and pre-beta particle formation by serum from human apolipoprotein A-I and apolipoprotein A-I/apolipoprotein A-II transgenic mice consistent with the latter being less effective for reverse cholesterol transport. *Biochemistry*. 1997;36:2243-2249.
29. Libby P, Sukhova G, Lee RT, et al. Cytokines regulate vascular functions related to stability of the atherosclerotic plaque. *J Cardiovasc Pharmacol*. 1995;25:S9-S12.
30. Rong JX, Li J, Reis ED, et al. Elevating high-density lipoprotein cholesterol in apolipoprotein e-deficient mice remodels advanced atherosclerotic lesions by decreasing macrophage and increasing smooth muscle cell content. *Circulation*. 2001;104:2447-2452.
31. Galis ZS. Atheroma morphology and mechanical strength: looks are important, after all. Lose the fat. *Circ Res*. 2000;86:1-3.
32. Galis ZS, Sukhova GK, Lark MW, et al. Increased expression of matrix metalloproteinases and matrix degrading activity in vulnerable regions of human atherosclerotic plaques. *J Clin Invest*. 1994;94:2493-2503.
33. Moreno PR, Falk E, Palacios IF, et al. Macrophage infiltration in acute coronary syndromes: implications for plaque rupture. *Circulation*. 1994;90:775-778.
34. Libby P, Geng YJ, Aikawa M, et al. Macrophages and atherosclerotic plaque stability. *Curr Opin Lipidol*. 1996;7:330-335.

**Long-Term Stable Expression of Human Apolipoprotein A-I Mediated by Helper-Dependent Adenovirus Gene Transfer Inhibits Atherosclerosis Progression and Remodels Atherosclerotic Plaques in a Mouse Model of Familial Hypercholesterolemia**

L. Maria Belalcazar, Aksam Merched, Boyd Carr, Kazuhiro Oka, Kuang-Hua Chen, Lucio Pastore, Arthur Beaudet and Lawrence Chan

*Circulation*. 2003;107:2726-2732; originally published online May 12, 2003;  
doi: 10.1161/01.CIR.0000066913.69844.B2

*Circulation* is published by the American Heart Association, 7272 Greenville Avenue, Dallas, TX 75231  
Copyright © 2003 American Heart Association, Inc. All rights reserved.  
Print ISSN: 0009-7322. Online ISSN: 1524-4539

The online version of this article, along with updated information and services, is located on the  
World Wide Web at:

<http://circ.ahajournals.org/content/107/21/2726>

**Permissions:** Requests for permissions to reproduce figures, tables, or portions of articles originally published in *Circulation* can be obtained via RightsLink, a service of the Copyright Clearance Center, not the Editorial Office. Once the online version of the published article for which permission is being requested is located, click Request Permissions in the middle column of the Web page under Services. Further information about this process is available in the [Permissions and Rights Question and Answer](#) document.

**Reprints:** Information about reprints can be found online at:  
<http://www.lww.com/reprints>

**Subscriptions:** Information about subscribing to *Circulation* is online at:  
<http://circ.ahajournals.org/subscriptions/>